Pricing analysis of wind power derivatives for renewable energy risk management

Pricing Analysis of Wind Power Derivatives for Renewable Energy Risk Management*

Takashi Kanamura,† Lasse Homann,‡ Marcel Prokopczuk§,¶

Tuesday 31st August, 2021

ABSTRACT

The objective of this study is to analyse the theoretical pricing of wind power derivatives, which is important for renewable energy risk management but has a problem in the pricing due to the illiquidity of the assets and to show the application of the theory to the practical implementation of the pricing. We make three contributions to the literature. First, to the best of our knowledge, we are the first to conduct a detailed econometric analysis of the wind power futures underlying, i.e., the electricity production based on windmills, resulting in strong support of seasonality and mean reversion in the logit transformed wind power load factors. Second, after proposing a new model of wind power load factors based on the econometric findings, we analyse the theoretical prices of wind power futures and call option contracts to which the good-deal bounds pricing within an illiquid market situation is applied as well as we show the application of the theory to the practical pricing with the illiquidity. Third, our empirical pricing analysis shows that theoretical wind power futures prices derived using seasonal modelling more accurately reflect reality than those derived without seasonality compared to market observations, resulting in the importance of seasonality modelling in theoretical wind power derivatives pricing. Because the upper and lower price boundaries represent the selling and the buying prices in the incomplete market, the pricing of the short position is more affected by the seasonality than the pricing of the long position. Finally, we discuss the applications of the results obtained in this study.

Key words: Wind power, load factor, good-deal bounds, futures and options, mean reversion, seasonality

JEL Classification: G13, L94, Q42

*Views expressed in this paper are those of the authors. All remaining errors are ours. We are grateful to two anonymous referees, Jinyue Yan (Editor-in-Chief) and Hong-xing Yang (Editor) for their valuable comments and suggestions.

†Graduate School of Advanced Integrated Studies in Human Survivability (GSAIS), Kyoto University, 1, Yoshida-Nakaadachi-cho, Sakyo-ku, Kyoto 606-8306, Japan, E-mail: kanamura.takashi.3u@kyoto-u.ac.jp

‡Institute of Finance and Commodity Markets, Leibniz University Hannover, Königsworther Platz 1 30167 Hannover, Germany, e-mail: homann@fcm.uni-hannover.de

§Institute of Finance and Commodity Markets, Leibniz University Hannover, Königsworther Platz 1 30167 Hannover, Germany, e-mail:prokopczuk@fcm.uni-hannover.de

¶ICMA Centre, University of Reading, Whiteknights, Reading, RG6 6BA, U.K.

1. Introduction

Wind power has become an important production type in the German electricity market and enjoys special status together with other renewables in the course of the "Energiewende", i.e., the transformation to renewable electricity production.[1] With the growing economic importance of wind power comes challenges in operational production planning of wind farm owners along with incentives to hedge the related financial risks.

Wind power projects, which are thus becoming an increasingly important part of the power industry, are subject to risks related to natural phenomena such as wind speed that varies stochastically. Thus, risk management tools for the wind power business are needed in order to make the sector sustainable. For example, during the cold wave blackout in Texas on February 15, 2021, about 16 GW of capacity was lost from renewable energy supplies, mainly from wind production. It is therefore indisputable that there is a strong need for weather risk management for wind power generation. Wind power risk management products generally have sellers and buyers, with the sellers often being the financial institutions as the risk takers and the buyers often being the wind power producers as the risk hedgers. Therefore, it is important to share the results of research on wind power risk management methods not only with economically-minded readers, such as researchers and practitioners in financial institutions, who may be sellers of the risk management products, but also with technologically-minded readers such as researchers and engineers in wind power generation companies, who need to manage wind power risks and who may be buyers of the risk management products for future applications.

At a background to these market and industry developments, the European Energy Ex-

[1] Although wind power generation is an immediate and effective measure against global warming, subsidies such as the German feed-in tariff have recently been reduced because the amount of wind power has rapidly increased. New financing in the wind energy sector during 2010 - 2019 in Europe peaked at 32.7 €bn in 2016 and was at 19.1 €bn in 2019 (WindEurope, 2020).

change (EEX) started offering wind power futures in October 2016. Wind power futures are designed to allow market participants to hedge the volume risks that are related to the electricity generation by windmills. The settlement is conducted financially and the underlying is a model-based load factor calculated by EuroWind, which uses meteorological data from the German Weather Office (DWD) and the Central Institution for Meteorology and Geodynamics (ZAMG) in combination with a turbine database to estimate wind power generation in Germany and Austria. The settlement is determined by the average wind power load factor times the total number of hours within the respective delivery period. EEX offered contracts with weekly, monthly, quarterly, and yearly delivery periods.[2]

In order to actually trade wind power futures on the EEX, it is necessary to determine a theoretical price, but there are two obstacles to reaching this goal. The first of these is the modelling of the wind power load factor, which is the underlying variable of the wind power futures contract. This requires a detailed econometric analysis using historical wind load factor data. Secondly, the low illiquidity of the wind power futures market makes pricing difficult since the market incompleteness of the illiquid contract needs to be taken into account in the pricing approach.

In this paper, we aim to deal with these two topics. We first conduct an econometric analysis of the underlying variable of the wind power futures contract, the amount of electricity produced by wind. We then propose a new model of wind power load factors based on our econometric findings, and analyse theoretical prices of wind power futures and option contracts by suggesting a valuation methodology which is based on the concept of good-deal bounds for incomplete markets.

[2]The wind power futures were delisted at EEX in August 2020 due to the split of the Austrian and German bidding zones and due to very low trading volumes. We believe that these low trading volumes do not reflect the fact that there is no demand for such a contract, but mostly the reluctance of market participants to trade something which is very difficult to assess. As such, we believe that our study might contribute to a better understanding of wind power futures and their acceptance in the electricity industry.

In the current market environment, the liquidity of wind power derivatives is very low, and, thus, an appropriate theoretical framework is needed. The pricing of weather derivatives has been previously examined in the literature. According to asset pricing theory, the price of an asset is represented by the expected value of the stochastic cash flows it will generate in the future, discounted by a stochastic discount factor (SDF). When pricing traded financial assets in liquid markets it is safe to assume market completeness, which yields a uniquely determined SDF. However, the market for weather derivatives in general, and for wind power futures in particular, is highly illiquid and thus the SDF is not uniquely determined. To overcome this problem, Cao and Wei (2004) calculate the price of temperature derivatives based on a SDF obtained from the assumed utility function and the optimal consumption of a representative agent. Davis (2001) analyses derivatives written on accumulated heating degree days using the SDF of an agent with a log utility function whose optimal consumption is proportional to the payoff of the derivatives. Brockett, Wang, Yang, and Zou (2006) use mean–variance utility and apply the indifference pricing approach to the valuation of weather derivatives. Similarly, Lee and Oren (2009) derive an equilibrium pricing model for weather derivatives in a multi-commodity setting, but it is assumed that all market participants are expected utility maximisers. While these methods are powerful for pricing illiquid assets, they need assumptions about the specific utility function of the trader. Using a different approach, Platen and West (2004) propose a fair pricing of weather derivatives where the growth optimal portfolio is used as a benchmark or numeraire. However, this also makes a strong assumption with respect to the existence of the numeraire. In contrast, the good-deal bounds approach of Cochrane and Saa-Requejo (2000) does not rely on any such assumptions and only places exogenous constraints on the variance of the stochastic discount factor. Kanamura and Ōhashi (2009) apply this approach to summer day options.

However, the pricing of wind power futures has not received a lot of attention in the literature, probably because the wind power futures were only introduced at the EEX for the

first time in 2016. Benth and Šaltytė Benth (2009) consider wind speed futures and suggest a pricing approach under the risk neutral measure where daily average wind speeds are dynamically modelled by a continuous-time autoregressive model with seasonal mean and volatility. Alexandridis and Zapranis (2013) present a pricing formula of futures contracts written on the cumulative average wind speed and the Nordix wind speed index also under the risk neutral measure. Benth and Pircalabu (2018) derive prices for wind power futures in the framework of no-arbitrage pricing by proposing a non-Gaussian Ornstein–Uhlenbeck model for the wind power load factor series. Finally, Benth, Di Persio, and Lavagnini (2018) construct and price a European put-type quanto option in the wind energy markets under the assumption of the identification of the risk neutral measure with the physical measure that allows the buyer to hedge against low prices and low wind power production. These studies assume complete markets whose liquidity is high. But in the case of wind power futures liquidity is low and, thus, the market is incomplete. As a way to avoid using very strong assumptions such as risk-neutral valuation, Gersema and Wozabal (2017) propose a stylised equilibrium pricing model featuring two representative agents and analyse equilibrium prices as well as the mechanics behind risk premia for wind power futures by using monthly EEX and Nasdaq OMX wind futures. However, their model is based on Bessembinder and Lemmon (2002) where it is assumed that the agents' expected utility is linearly dependent on the expected profit and the variance. This approach requires assumptions about the utility function. Recently Rodríguez, Pérez-Uribe, and Contreras (2021) designed and priced an up-and-in European wind put barrier option using Monte Carlo simulation as the average value of the simulations. Hess (2021) proposed a new model for the pricing of wind power futures written on the wind power production index under a risk neutral measure. The existing theoretical pricing methods usually assume complete markets which exhibit high liquidity. However, the market for wind power futures is incomplete due to its low liquidity. In this light, it is worthwhile to apply the good-deal bounds pricing method of Cochrane and Saa-Requejo (2000) to wind power futures. This approach is

based on relatively weak assumptions that only place exogenous constraints on the variance of the stochastic discount factor. Furthermore, the existing literature mentioned above including recent studies (Rodríguez, Pérez-Uribe, and Contreras, 2021; Hess, 2021) does not conduct detailed empirical analyses of wind power load factors, which are the underlying variables of wind power futures contracts. Since wind power futures prices are based on wind power load factors, such an analysis is one of important applied value because one cannot obtain correct wind power futures prices without an appropriate stochastic model.

This paper focuses on theoretical wind power derivatives pricing in an incomplete market setting, which takes the market illiquidity currently observed in the market into account, in order to determine theoretical prices of wind power futures and wind power call options newly designed by incorporating the seasonality of wind power generation. The contribution of our paper is thus threefold. To support our modelling, for the first time, we first conduct a detailed econometric analysis of the wind power load factor which is the underlying of the wind power futures. Second, based on the econometric findings, we conduct a pricing analysis of wind power derivatives by providing a pricing model of wind power derivatives based on good-deal bounds within an incomplete market setting as well as we show the application of the theory to the practical implementation of the pricing. Third, we illustrate the adverse consequences of ignoring seasonality in the model and discuss seasonality model risk premiums by putting our model to the data, using the wind power load factor to estimate the model parameters, and then obtaining wind futures and call option good-deal price boundaries.

The remainder of this paper is organised as follows. Section 2 conducts an econometric analysis of the wind power futures underlying time series, i.e., the amount of electricity production from windmills. Section 3 proposes a new model of wind power load factors based on the empirical findings and derives the partial differential equation of wind power derivatives price boundaries in theory based on the idea of the good-deal bounds in incomplete markets. Section 4 presents an empirical pricing analysis to calculate theoretical wind power derivatives

price boundaries and examines seasonality model risk premiums driven by the differences between wind power derivatives prices with and without seasonality in the model as well as it shows the application of the theory to the practical implementation of the pricing and discusses the application of the results obtained in this study. Section 5 concludes.

2. Econometric Analysis

2.1. Data

The wind index data used in this paper was obtained from Eurowind. The index is reported on an hourly basis covering the period of January 1980 through December 2017 and represents the fraction of wind power production relative to total capacity, i.e., it is bounded between 0 and 100%. This index is referred to as "a wind power load factor". The wind power load factor is strongly influenced by weather conditions since the amount of electricity produced depends on the wind speed. The minimum and maximum of the hourly series is 0.13% and 77%, respectively. To match the delivery periods of the futures contracts, the index is aggregated to weekly and monthly means. Additionally, the daily mean series is considered, since it provides further insights into the behaviour of the index. Table 1 presents descriptive statistics of the daily average wind power load factor (DWPLF), of the weekly average wind power load factor (WWPLF), and of the monthly average wind power load factor (MWPLF). The time series mean is 22.29% and the standard deviation is 14.61, 10.27, and 7.02 with 13,880, 1,983 and 456 observations for the daily, weekly, and monthly series, respectively. All three series are left-skewed and normality is rejected in every case. The empirical distribution functions are shown in Figure 1.

Noticeable, the distributions of the considered aggregations of the wind power index have similar characteristics as those of wind speed data in existing studies (e.g., Brown, Katz,

	Mean	Median	Max	Min	SD	Skew	Kurt	AD
DWPLF	22.29	18.34	75.08	0.88	14.61	1.17	0.93	≤ 0.01
logit DWPLF	-1.44	-1.49	1.10	-4.72	0.88	0.25	-0.17	≤ 0.01
deseas DWPLF	0	-0.03	2.44	-3.56	0.83	0.08	-0.15	≤ 0.01
WWPLF	22.29	20.11	62.42	5.48	10.27	1.03	0.74	≤ 0.01
logit WWPLF	-1.34	-1.38	0.51	-2.85	0.59	0.34	-0.17	≤ 0.01
deseas WWPLF	0	-0.01	1.48	-1.68	0.52	0.01	-0.17	0.06
MWPLF	22.29	20.99	48.96	9.54	7.02	0.98	0.92	≤ 0.01
logit MWPLF	-1.29	-1.33	-0.04	-2.25	0.39	0.44	0.06	≤ 0.01
deseas MWPLF	0	0.00	0.85	-0.91	0.27	0.14	0.32	0.1

Table 1. Descriptive Statistics

This table presents basic descriptive statistics. Reported are the mean, median, maximum, minimum, standard deviation, skewness, and kurtosis. To check for normality the test following Anderson and Darling (1952) is used. The p-values are reported in the column AD.

and Murphy, 1984; Bivona, Bonanno, Burlon, Gurrera, and Leone, 2011; Alexandridis and Zapranis, 2013). In the literature, several distributions have been fitted to average hourly wind speed data, including the gamma distribution (Sherlock, 1951), the inverse Gaussian distribution (Bardsley, 1980), the squared normal distribution (Carlin and Haslett, 1982), log-normal distributions (Luna and Church, 1974; Torres and De Francisco, 1998), the Chi-square (Dorvlo, 2002), and the Weibull distribution (Hennessey, 1978; Brown, Katz, and Murphy, 1984; Akpinar and Akpinar, 2005; Torres, Garcia, De Blas, and De Francisco, 2005; Bivona, Bonanno, Burlon, Gurrera, and Leone, 2011, among others). Among these, the Weibull distribution has proven itself to fit the average hourly wind speed data best.

Although it is tempting to transfer the results of these studies on wind speeds to the wind power load factors, one has to keep in mind that, while being related, these are different things, wind speed vs. the amount of electricity produced from windmills. Moreover, the support of the wind power load factor, in the following denoted by L_t, is bounded from above by 1 (or 100%), whereas wind speeds are not. To overcome this problem, we consider a simple and well known data logit transformation. The resulting variable can be modelled continuously

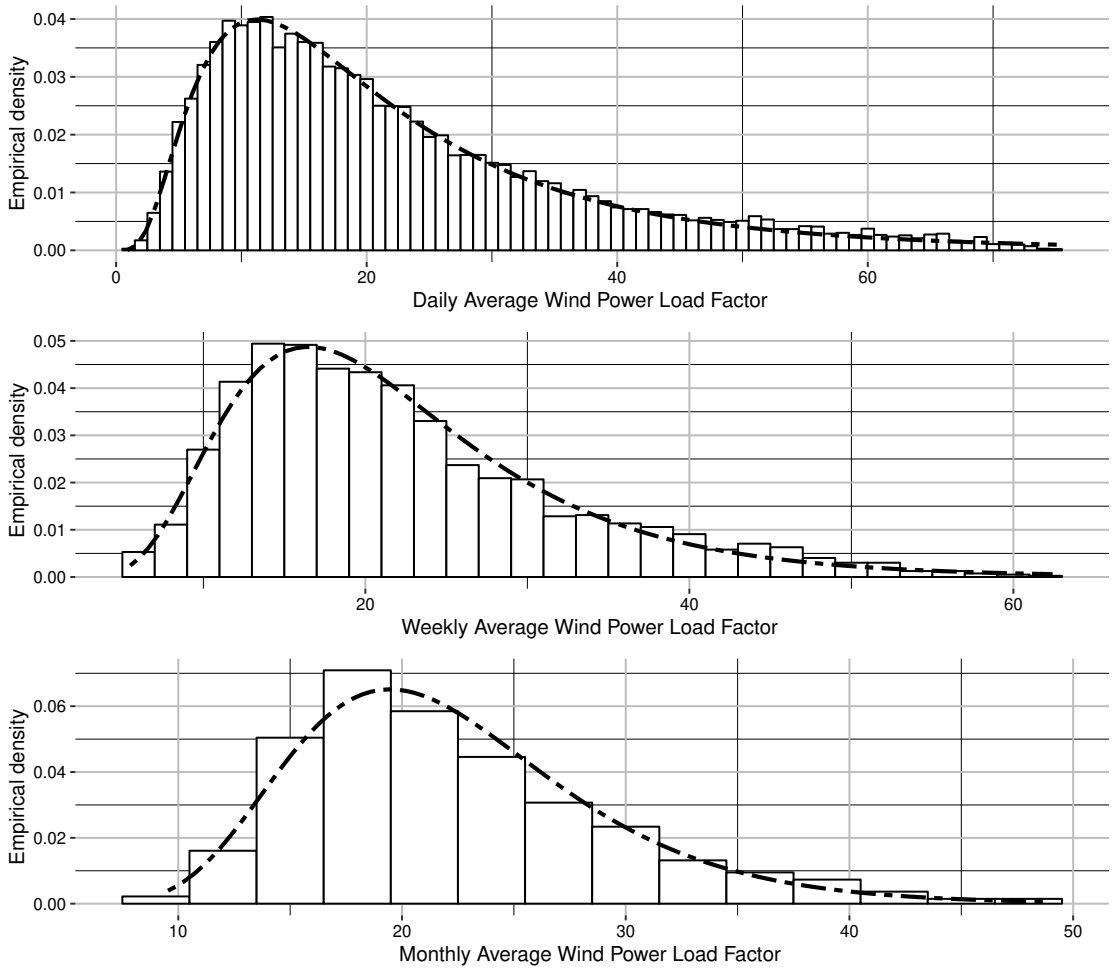

Figure 1. Empirical Distributions

for the real numbers, which guarantees that the back-transformed fitted values lay within the interval [0, 1]. The transformation function is given by

$$X_t = -\log\left(\frac{1}{L_t} - 1\right), \tag{1}$$

where X_t denotes the respective series, i.e., DWPLF, WWPLF, and MWPLF for the daily, weekly, and monthly series, respectively. Summary statistics of the logit-transformed series can also be found in Table 1. Although the transformed series are more symmetric, normality is still rejected at any common significance level. In addition to the transformation, the daily

series are roughly split into three equally long periods to fit and analyse models independently for each subsample. The considered periods are 1970–1992, 1993–2005, and 2006–2017.

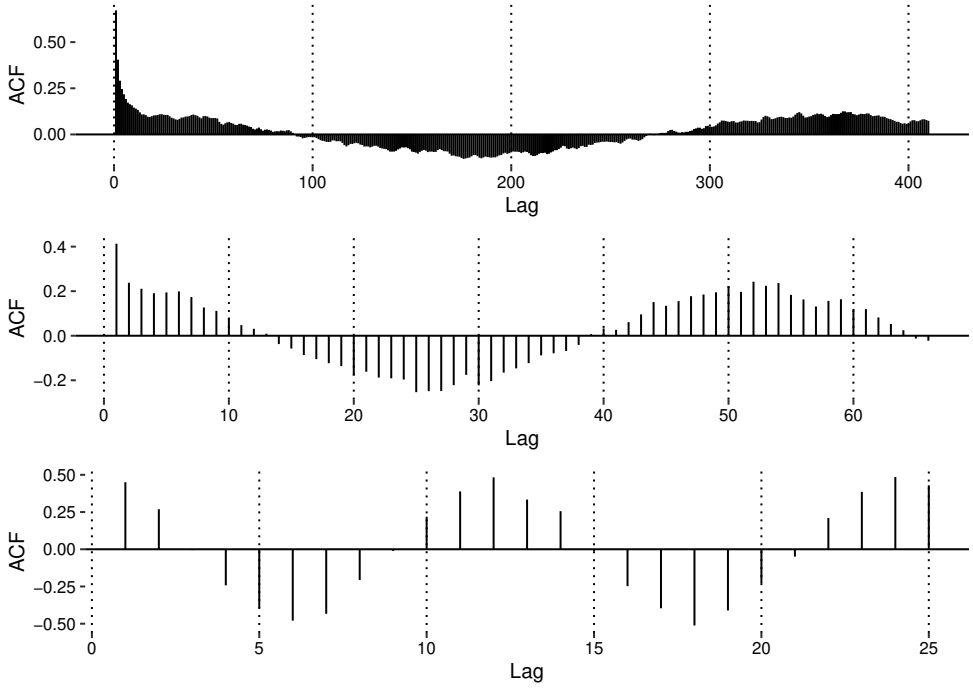

Figure 2. Correlogram of Raw Series

This figure shows the correlogram of the raw series DWPLF, WWPLF, MWPLF (from top to bottom). For the logit-transformed series the correlograms exhibit similar patterns.

2.2. A mean model for wind power load factors

Figure 2 shows the empirical autocorrelations of DWPLF, WWPLF, and MWPLF. It can be seen that all series have a cyclical pattern in the autocorrelations caused by annual seasonality in the data. The pattern is preserved in the logit-transformed data. The seasonal pattern is modelled continuously throughout the year by fitting the Fourier series given by

$$S_t^\tau = a_0^\tau + \sum_{k=1}^{K} a_k^\tau \sin\left(\frac{2\pi t k}{h^\tau}\right) + b_k^\tau \cos\left(\frac{2\pi t k}{h^\tau}\right), \tag{2}$$

where S_t^τ is the annual seasonal component of time series τ and a_0^τ is the time series average. Since we have daily, weekly and monthly data, h^τ is chosen to be 365.25, 52.179, and 12, respectively. K is the number of Fourier terms and for the following is set to be 1. The harmonic regression is preferred to an estimation using dummy variables since fewer parameters have to be estimated. We estimate the time series average a_0^τ and the coefficients a_1^τ and b_1^τ using least squares. The estimated coefficients along with their standard errors can be found in Table 2. A time series plot for the daily, weekly and monthly series along with the fitted seasonal functions and the residual series can be found in Figure 3. We also present summary statistics for the deseasonalised series in Table 1.

	$\hat{a_0^\tau}$	$\hat{a_1^\tau}$	$\hat{b_1^\tau}$
logit DWPLF	-1.439	0.048	0.406
	(≤ 0.001)	(≤ 0.001)	(≤ 0.001)
logit WWPLF	-1.339	0.072	0.391
	(0.012)	(0.016)	(0.016)
logit MWPLF	-1.289	0.145	0.373
	(0.016)	(0.018)	(0.018)

Table 2. Seasonal Adjustment

2.3. Results

In each estimation, the residuals resemble the deseasonalised series, which are in the following modelled with the class of stationary ARMA(p,q) processes.[3] To fit the ARMA(p,q) models to the deseasonalised series we use the method of maximum likelihood. Further, we estimate the optimal number of p and q with the Bayesian information criterion (BIC). Note that the monthly series does not show a significant dependency structure and hence no time series model is fitted. In addition to the model chosen by the information criterion, AR(1)-models

[3]Standard unit root tests are applied to all residual series, which are found to be stationary.

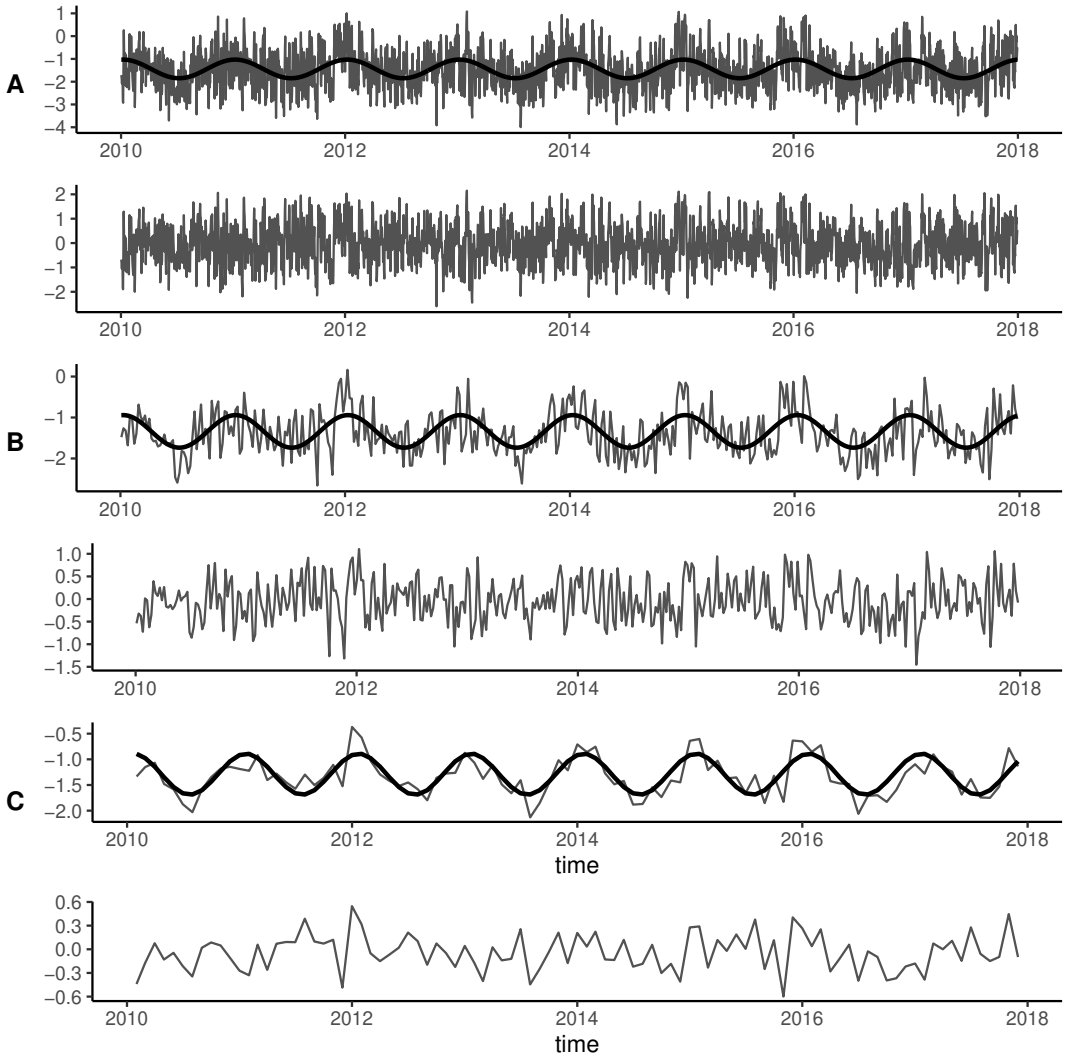

Figure 3. Time Series Plots

This figure shows the time series plot of the logit-transformed series DWPLF (A), WWPLF (B) and MWPLF (C), their seasonal component (thick black line), and their seasonal adjusted series (below each original series).

		LB_5	LB_{12}	LB_5^2	LB_{12}^2	AD	$KPSS$
Daily	full sample						
	ARMA(2,2)	0.11	0.21	$\leq$ **0.01**	$\leq$ **0.01**	$\leq$ **0.01**	0.24
	AR(1)	$\leq$ **0.01**	$\leq$ **0.01**	$\leq$ **0.01**	$\leq$ **0.01**	$\leq$ **0.01**	0.37
	1980 - 1992						
	ARMA(1,1)	**0.04**	**0.02**	**0.03**	0.10	**0.02**	0.25
	AR(1)	$\leq$ **0.01**	$\leq$ **0.01**	**0.01**	**0.04**	0.11	0.49
	1993 - 2005						
	ARMA(1,3)	0.21	0.80	$\leq$ **0.01**	$\leq$ **0.01**	**0.02**	0.62
	AR(1)	$\leq$ **0.01**	$\leq$ **0.01**	$\leq$ **0.01**	$\leq$ **0.01**	**0.03**	0.62
	2006 - 2017						
	ARMA(1,1)	0.07	0.06	0.14	0.13	**0.03**	0.47
	AR(1)	$\leq$ **0.01**	$\leq$ **0.01**	0.15	0.21	0.13	0.71
weekly	MA(1)	0.93	0.95	$\leq$ **0.01**	$\leq$ **0.01**	0.11	0.80
monthly	-	0.72	0.82	**0.02**	0.06	0.10	0.38

Table 3. Test Results

are fitted to the daily series and its subperiods, as the AR(1)-model is particularly simple and parsimonious.

Residuals are then investigated, to see whether they are white noise. To test for remaining serial correlation we apply the Ljung–Box (LB) test (Ljung and Box, 1978). Additionally, we also check for autoregressive conditional heteroscedasticity by applying the same test to the squared residuals. Lastly, to assess the assumption of normally distributed errors we employ the Anderson–Darling (AD)-test (Anderson and Darling, 1952) and the KPSS-test (Kwiatkowski, Phillips, Schmidt, and Shin, 1992). Table 3 presents the p-values for each test and model, respectively. For the daily series, the information criterion chooses higher-order ARMA models, but the LB test finds evidence for remaining dependencies for the ARMA(1,1) model estimated for the subperiod 1980 through 1992. However, the highest remaining residual autocorrelations are below 0.025, so that although some remaining dependencies are found, we consider the model for reasons of parsimony. Similarly, the LB test rejects the null for all considered AR(1) models at the 1%-significance level. The remaining significant autocorrelations are larger compared to those of the higher-order ARMA models

and vary between 0.05 and 0.1 within the first two lags. Thus, in the spirit of parsimony and to avoid overly complex pricing models with many free parameters, an AR(1) might be preferred. Regarding the weekly and monthly data, the LB test does not find evidence for remaining correlation in the data. Further discussions regarding the volatility process are provided in Appendix A.

3. The Derivatives Pricing Model

3.1. A new model of wind power load factors

The econometric analysis in Section 2 supports the modelling framework in which the logit transformed wind load factors follow a mean-reverting process with a mean that has a sinusoidal yearly cycle. Let X_t represent the inverse transformation of the logit model for the load factor L_t as in Equation (1). We propose a new model of wind power load factor (L_t) in which X_t follows a mean-reverting process in continuous time with seasonality:

$$dX_t = (\mu_X(t) - \lambda_X X_t)dt + \sigma_X dv_t, \tag{3}$$

$$\mu_X(t) = \theta_1 + \theta_2 \sin(\omega t) + \theta_3 \cos(\omega t), \tag{4}$$

with v_t being a standard Brownian motion. Note that L_t is an increasing function of X_t.

3.2. Design of wind power derivatives

To determine theoretical prices of wind power derivatives, we define a new variable: I_t, the accumulated average load factor within the contract period, which is expressed by

$$I_t = \int_0^t L_\tau d\tau. \tag{5}$$

The futures price $\underline{D}(S,X,I,T)$[4] is in theory determined by the underlying average wind load factor per contract period, which is represented by the average of I_t at maturity T:

$$\underline{D}(S,X,I,T) = \frac{I_T}{T}. \tag{6}$$

We also consider a European wind power call option with strike price K whose theoretical price $\underline{D}(S,X,I,T)$ based on a wind power futures as underlying is given by:[5]

$$\underline{D}(S,X,I,T) = \max\left(\frac{I_T}{T} - K, 0\right). \tag{7}$$

Note that a quoted 1 percentage point wind power load factor is equivalent to 1 €/h.

3.3. Good-deal bounds pricing for wind power derivatives

According to asset pricing theory, the price of an asset, such as a wind power derivative, is expressed as the expected value at the present time of the future cash flows generated by the asset, discounted by the SDF. In the case of wind power derivatives, the future cash is expressed in terms of $\underline{D}(S,X,I,T)$. Therefore, the question is how to characterise and model

[4] As explained in the next subsection, since good-deal bounds pricing uses the stock price S as the asset of a complete market, $\underline{D}$ includes S.

[5] Wind power call options have not been traded in the market so far. But when the liquidity of wind power futures increases, it can be expected that the options will be introduced at the market.

the SDF. We use the good-deal bounds method as one of the methods for characterising the SDF, especially as it is applicable in illiquid markets and does not require strong assumptions such as specific utility functions. Following Kanamura and Ōhashi (2009), we derive good-deal bounds pricing formulas for wind power futures and options. In order to characterise the SDF of good-deal bounds, a highly liquid market, i.e., a complete market, is required as a reference for the illiquid market of wind power derivatives. We assume that the complete market asset is a stock index (S_t) whose price follows a simple lognormal process:

$$\frac{dS_t}{S_t} = \mu_s dt + \sigma_s dw_t \tag{8}$$

where both μ_s and σ_s are constant and w_t is again a standard Brownian motion. Note that under this formulation, the market price of risk ϕ for w_t is given by $\phi = \frac{\mu_s - r}{\sigma_s}$ where r is a risk free rate and that $E[dw_t dv_t] = \rho_X dt$. Following the approach outlined in Kanamura and Ōhashi (2009), we calculate the lower price boundaries of a wind power derivative $\underline{D}_t$ at time t by using the good-deal bounds pricing. The lower boundary of the derivatives price can be obtained by selecting the stochastic discount factor (SDF) Λ_t in an incomplete market so that the total present expected value of future cash flows of x_s^c and x_T^c discounted by the SDF, is minimised. Equation (10) represents the stochastic process of Λ_t which is the sum of the stochastic process of the complete market SDF, Λ_t^*, as shown in Equation (11) and the incomplete market noise dz_t with v as a volatility parameter. Note that $dv_t = \rho_X dw_t + \sqrt{1-\rho_X^2} dz_t$. Equation (12) is the good-deal condition that limits the SDF with an exogenous Sharpe ratio of A.

$$\underline{D}_t = \min_{\{\Lambda_s, t \le s \le T\}} E_t \left[\int_t^T \frac{\Lambda_s}{\Lambda_t} x_s^c ds + \frac{\Lambda_T}{\Lambda_t} x_T^c \right], \tag{9}$$

$$\text{s.t. } \frac{d\Lambda_t}{\Lambda_t} = \frac{d\Lambda_t^*}{\Lambda_t^*} - v dz_t, \tag{10}$$

$$\frac{d\Lambda_t^*}{\Lambda_t^*} = -r dt - \phi dw_t, \tag{11}$$

$$\frac{1}{dt}E_t\left[\frac{d\Lambda_t^2}{\Lambda_t^2}\right] \leq A^2. \tag{12}$$

Similarly, the upper boundaries of the prices are obtained by replacing the minimisation with the maximisation in Equation (9). Suppose that the maximum Sharpe ratio after introducing a new derivative is given by A. Suppose also that the stock price S_t and the wind power load factor related variable X_t are given by Equations (8) and (3), respectively. Denote by X_t, the wind power load factor related variable that determines the wind power derivatives payoff I_T at maturity T. Then, the good-deal bounds upper and lower price boundaries of wind power load factor derivatives are given by the solutions of the following partial differential equation:

$$\begin{aligned}
&-r\underline{D}+\frac{\partial \underline{D}}{\partial t}+\frac{1}{2}\sigma_s^2S^2\frac{\partial^2\underline{D}}{\partial S^2}+\frac{1}{2}\sigma_X^2\frac{\partial^2\underline{D}}{\partial X^2}+\rho_X\sigma_s\sigma_X S\frac{\partial^2\underline{D}}{\partial X\partial S}+\frac{dI}{dt}\frac{\partial \underline{D}}{\partial I}\\
&=-rS\frac{\partial \underline{D}}{\partial S}+\left(\frac{\mu_s-r}{\sigma_s}\rho_X\sigma_X-\mu_X(t)+\lambda_X X_t+\eta\sqrt{A^2-\left(\frac{\mu_s-r}{\sigma_s}\right)^2}\sigma_X\sqrt{1-\rho_X^2}\mathrm{sgn}\left(\frac{\partial \underline{D}}{\partial X}\right)\right)\frac{\partial \underline{D}}{\partial X}
\end{aligned} \tag{13}$$

with the terminal payoff of the futures and the call option in Equations (6) and (7), respectively, and where $\eta=+1$ and -1 generate the lower and upper price boundaries, respectively. K represents the strike price of the call option. Note that we set $x_s^c=0$ for European-type wind power derivatives pricing. The details of the derivation of Equation (13) from Equations (9) to (12) are offered in Appendix A of Kanamura and Ōhashi (2009). First, Equation (6) or (7) is set to the payoff at $t=T(>0)$, the maturity of the derivative. The partial differential Equation (13) is then discretised and solved backward from $t=T$ in time to obtain the price of the derivative at $t=0$ numerically by using the finite difference method. Note that from Equation (5) we have $\frac{dI}{dt}=L$ in Equation (13). Thus the upper and lower price boundaries of wind power load factor derivatives $\underline{D}_t$ including wind power futures and call options can be obtained by good-deal bounds. It is important to notice that as the practical implementation of good-deal bounds, Cochrane and Saa-Requejo (2000) suggest that traders can use the bounds as buy and sell points. Therefore, the upper and lower boundaries of the wind power derivative

price obtained in this calculation correspond to the selling price and the buying price of the wind power derivative for the seller and the buyer, respectively. Lastly note that since the marginal costs of wind power are effectively zero, wind power is at the very beginning of the merit order curve. Therefore, time-varying demand does not really matter as long as it is higher than wind capacity.

Based on the theory of Section 3 above, after estimating the model parameters using data, the next section will conduct pricing analysis of wind power derivatives as well as show the application of the theory of wind derivatives pricing to the actual implementation of the pricing with the illiquidity.

4. Empirical Pricing Analysis

4.1. Model parameter estimation and wind power derivatives pricing

We use data covering the period from January 1, 2010 to December 31, 2017. The hourly wind index data is transformed to the daily level by using the simple average. We use daily stock price index data of the major German stock index, DAX, which is obtained from Bloomberg. We now estimate the parameters of the wind power load factor model. Good-deal pricing evaluates the risk and return in the incomplete market from the wind power load factor by reference to the relationship between the risk and return of the German stock market. Thus, simultaneous estimation of the stock price that forms a complete market and the logit-transformed wind power generation load factor that forms an incomplete market is required. The discretised stochastic process of the stock index is given by

$$\Delta \log S_t = (\beta_0 - \frac{1}{2}\sigma_1^2) + \varepsilon_{1t}, \tag{14}$$

and the discretised model of X_t, the inverse transformation of the logit model for the load factor, is given by

$$\Delta X_t = \alpha_0 + \alpha_2 \sin(\omega t) + \alpha_3 \cos(\omega t) - \alpha_1 X_t + \varepsilon_{2t}. \tag{15}$$

Note that $\varepsilon_i = (\varepsilon_{1t}, \varepsilon_{2t}) \sim N(\mu_\varepsilon, \Sigma_\varepsilon)$, $\mu_\varepsilon = (0,0)$, and $\Sigma_\varepsilon = \begin{pmatrix} \sigma_1^2 & \rho\sigma_1\sigma_2 \\ \rho\sigma_1\sigma_2 & \sigma_2^2 \end{pmatrix}$. We simultaneously estimate the parameters by the method of maximum likelihood. The results are reported in Table 4. According to the standard errors in Table 4, σ_1, α_0, α_1, σ_2, and α_3 are statistically significant. Note that the results capture the mean reversion of the logit-transformed

Model Parameters	β_0	σ_1	α_0	α_1	σ_2	ρ	α_2	α_3
Estimates	0.0003	1.036E-02	-0.586	0.396	0.642	-0.011	0.017	0.163
Standard Errors	0.0002	1.324E-04	0.013	0.007	0.009	0.019	0.018	0.020
Loglikelihood	6.356E+03							
AIC	-1.270E+04							
SIC	-1.271E+04							

Table 4. Model Parameter Estimation with Seasonality

wind power load factor deviation from the mean because the estimate of α_1 (0.396) is greater than 0 and less than 1. The parameters (μ_s, σ_s, λ_X, σ_X, ρ_X, θ_1, θ_2, θ_3) of the continuous-time models in Equations (8) and (3) are obtained by integrating Equations (8) and (3) from t to $t+1$ and comparing the coefficients with the corresponding discrete-time models. We obtain

μ_S	σ_S	λ_X	σ_X	ρ_X	θ_1	θ_2	θ_3
0.0003	0.0104	0.5047	0.8085	-0.0115	-0.7465	0.0236	0.2079

Table 5. Continuous-Time Model Parameters with Seasonality

the following results:

$$
\begin{aligned}
&\mu_s = \beta_0, && \sigma_s = \sigma_1,\\
&\lambda_X = -\ln(1-\alpha_1), \;\; \sigma_X = \sigma_2\sqrt{\frac{2\ln(1-\alpha_1)}{(1-\alpha_1)^2-1}}, \;\; \rho_X = \frac{\sigma_1\sigma_2}{\sigma_s\sigma_X}\frac{\lambda_X}{1-e^{-\lambda_X}}\rho,\\
&\theta_1 = (\lambda_X\alpha_0)\frac{1}{1-e^{-\lambda_X}},\\
&\begin{pmatrix}\theta_2\\ \theta_3\end{pmatrix} = \frac{1}{B_1^2+B_2^2}\begin{pmatrix}\lambda_X B_1+\omega B_2 & -(\omega B_1-\lambda_X B_2)\\ \omega B_1-\lambda_X B_2 & \lambda_X B_1+\omega B_2\end{pmatrix}\begin{pmatrix}\alpha_2\\ \alpha_3\end{pmatrix}.
\end{aligned}
\tag{16}
$$

Note that $B_1 = \cos(\omega) - e^{-\lambda_X}$ and $B_2 = \sin(\omega)$ where we assume $\omega = 2\pi/365.25$. Table 5 reports the conversion results.

We now numerically compute theoretical wind power futures prices by using the partial differential equation in Equation (13) with the terminal payoff in Equation (6). A quoted 1 percentage point wind power load factor is equivalent to 1 €/h. For simplicity, we assume the risk free rate to be 0.00004 (1%/year). We calculate the wind power futures price as of December 31, 2017 with maturity January 31, 2018 as an example of peak season wind power generation: Equation (13), when discretised, becomes a relational equation of wind power futures prices connecting time t and time $t+1$ for any time t. Since the payoff of the wind power futures at maturity is predetermined by the contract in Equation (6), the current price of the wind power futures as of December 31, 2017 can be obtained by solving backward for time using Equation (13) from the value at maturity as of January 31, 2018. Figure 4 shows the lower boundary of the wind power futures price when the incomplete market demands three times the Sharpe ratio ($A = 3\phi$) in Equation (12). It can be seen that the impact of the initial

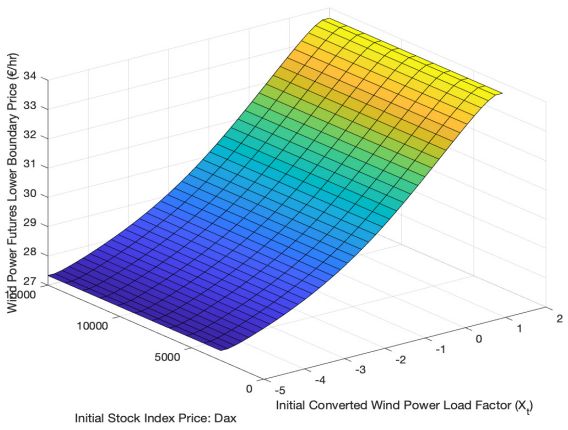

Figure 4. Wind power futures lower price boundary on December 31, 2017 for January 31, 2018 delivery. Note: $A = 3\phi$.

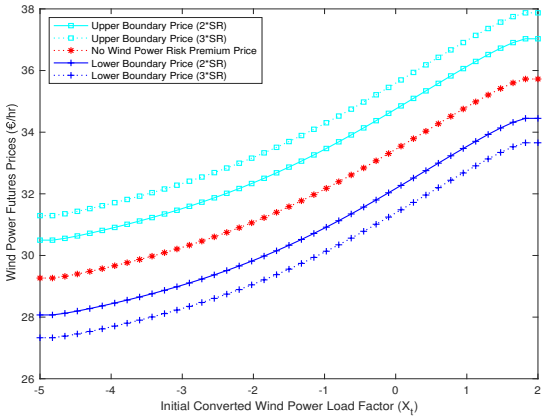

Figure 5. Wind power futures price boundaries on December 31, 2017 for January 31, 2018 delivery. Note: Dax S_t is 11,400 as an example.

stock price on the lower boundary of the wind power futures price is limited. Figure 5 shows the results for the case where the initial stock price is fixed at 11,400 and $A = \phi$ (No wind power risk premium), 2ϕ and 3ϕ, respectively. As a practical implementation of good-deal bounds, we were able to calculate the selling price, expressed as an upper price boundary, and the buying price, expressed as a lower price boundary, in the illiquid wind power futures market. In addition, we observe that the price boundary level of the wind power futures price changes according to the level of the Sharpe ratio, which represents the total return sought by the market participants due to the low liquidity of the wind power futures. Since the logit-transformed wind power load factor is positively related to the load factor of wind power generation, the futures price increases as the load factor of wind power generation increases. Considering that the final settlement price of wind power futures released by EEX for January 2018 is 35.63 (EEX, 2018a), it can be seen that the model provides a similar result. We also compute theoretical wind power futures prices as of June 30, 2018, with delivery July 31, 2018 as an example of the off-peak season of wind power generation. The results are reported in Figures 6 and 7. Again, considering that the logit-transformed wind power load factor is positively related to the load factor of wind power generation, the futures price increases as

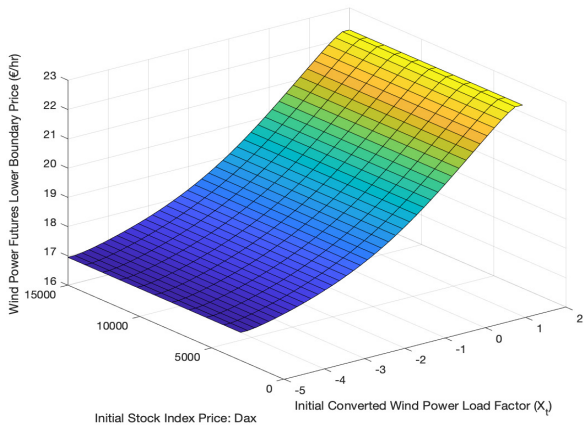

Figure 6. Wind power futures lower price boundary on June 30, 2018 for July 31, 2018 delivery. Note: $A = 3\phi$.

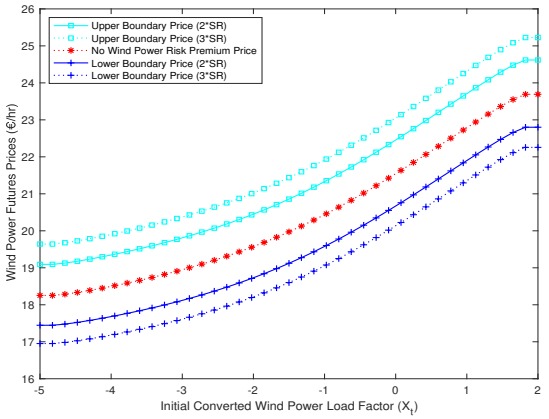

Figure 7. Wind power futures price boundaries on June 30, 2018 for July 31, 2018 delivery. Note: Dax S_t is 11,400 as an example.

the load factor of wind power generation increases which is the same as the example of peak season of wind power generation in Figures 4 and 5. The settlement price of wind power futures released by EEX for July 2018 was 10.48 (EEX, 2018b). It can be seen that the model is not too far from this observed price. Taking into account that wind resources in the summer of 2018 were 20% to 30% down compared to the normal years because of the heatwave in Western Europe, we can safely say that the results track well the seasonality effect of wind power futures.

We now consider the calculation of call options written on the wind power futures. We numerically calculate theoretical wind power call option prices on December 31, 2017 with delivery in January 31, 2018 by using the partial differential equation in Equation (13) with the terminal payoff in Equation (7) where we set the strike price to $K = 20\%$: Equation (13), when discretised, becomes a relational equation of wind power call option prices connecting time t and time $t+1$ for any time t. Since the payoff of the wind power call option at maturity is predetermined by the contract in Equation (7), the current price of the wind power call option as of December 31, 2017 can be obtained by solving backward for time using Equation (13) from the value at maturity as of January 31, 2018. Figure 8 shows the lower boundary of

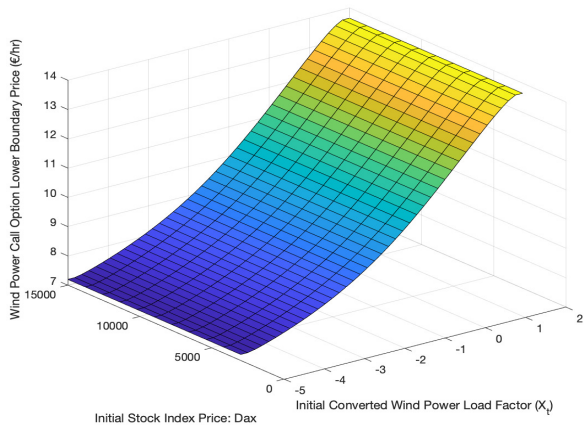

Figure 8. Wind power call option lower price boundary on December 31, 2017 for January 31, 2018 delivery. Note: $A = 3\phi$.

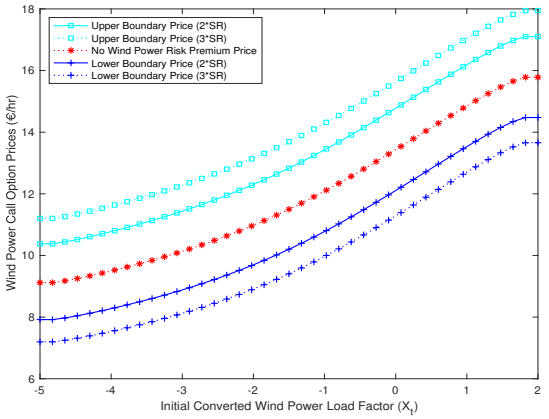

Figure 9. Wind power call option price boundaries on December 31, 2017 for January 31, 2018 delivery. Note: Dax S_t is 11,400 as an example.

the wind power call option price when the incomplete market demands three times the Sharpe ratio ($A = 3\phi$) in Equation (12). It can be seen that the impact of the initial stock price on the lower boundary of the wind power call option price is limited. Figure 9 shows the results for the case where the initial stock price is fixed at 11,400 and $A = \phi$ (No wind power risk premium), 2ϕ and 3ϕ, respectively. As a practical implementation of good-deal bounds, we were able to calculate the selling price, expressed as an upper price boundary, and the buying price, expressed as a lower price boundary, in the illiquid wind power call option market. In addition, we observe that the price boundary level of the wind power call option price changes according to the level of the Sharpe ratio, which represents the total return sought by the market participants due to the low liquidity of the wind power call option. One can observe that the option price increases as the wind load factor increases because the probability of exceeding 20%, i.e., -1.386 in X_t of the strike increases. As a second example during the off-peak period, we consider theoretical wind power call option prices on June 30, 2018 to be delivered at July 31, 2018. Figures 10 and 11 show similar results as for the peak wind power season in Figures 8 and 9 in the sense of the relationship of the prices and wind power load factors. However, the results also show that the option prices in the off peak are smaller than

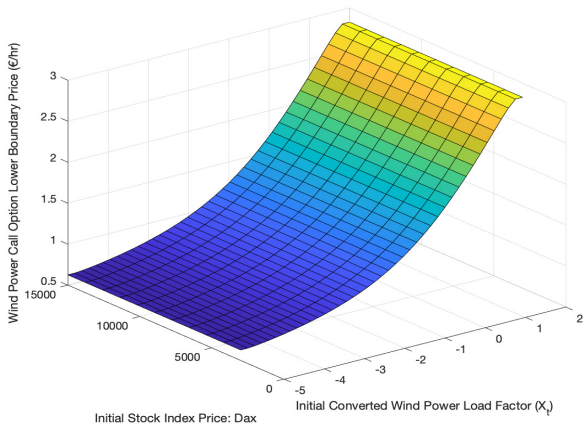

Figure 10. Wind power call option lower price boundary on June 30, 2018 for July 31, 2018 delivery. Note: $A = 3\phi$.

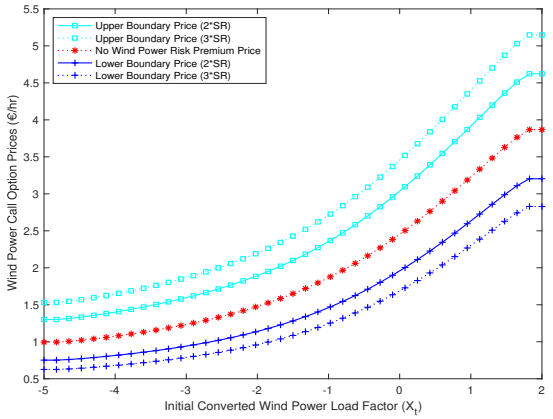

Figure 11. Wind power call option price boundaries on June 30, 2018 for July 31, 2018 delivery. Note: Dax S_t is 11,400 as an example.

the option prices in the peak period. This result reflects the importance of the inclusion of seasonality modelling in wind power derivatives.

4.2. Seasonality model risk premium

In order to further examine the importance of seasonality modelling in wind power derivatives, we consider the difference in the theoretical prices of wind power derivatives with and without seasonality modelling. We define the seasonality model risk premium (SMRP) by

$$\underline{SMRP}_t = \underline{D}^{\mathrm{w/S}} - \underline{D}^{\mathrm{w/oS}} \tag{17}$$

where superscripts w/S and w/oS represent wind power futures prices with and without seasonality, respectively. For wind power futures prices without seasonality, we estimate the converted wind load factor without seasonality in Equations (14) and (15) assuming that $\alpha_2 = \alpha_3 = 0$.

We report the estimated SMRP in Figures 12 and 13 by using theoretical wind power futures

Model Parameters	β_0	σ_1	α_0	α_1	σ_2	ρ
Estimates	0.0003	1.036E-02	-0.518	0.350	0.651	-0.007
Standard Errors	0.0002	1.336E-04	0.013	0.007	0.009	0.019
Loglikelihood	6.315E+03					
AIC	-1.262E+04					
SIC	-1.263E+04					

Table 6. Model Parameter Estimation without Seasonality: According to the corresponding standard errors, σ_1, α_0, α_1, σ_2, and α_3 are statistically significant.

μ_S	σ_S	λ_X	σ_X	ρ_X	θ_1
0.0003	0.0104	0.4314	0.7951	-0.0075	-0.6380

Table 7. Continuous-Time Model Parameters without Seasonality

prices on December 31, 2017 to be delivered on January 31, 2018 and on June 30, 2018 to be delivered on July 31, 2018, as examples of peak and off-peak wind power generation, respectively. Figure 12 suggests that when the load factor of wind power generation is low, the SMRP is big, and vice versa. In Germany, the load factor of wind power generation is high and low in winter and summer, respectively. Thus, when hedging the wind power load factor in the summer season with futures, it is important to consider the seasonality when modelling the load factor from the viewpoint of the SMRP. The good-deal bounds can be interpreted as the upper price limit being the selling price of the seller and the lower price limit being the buying price of the buyer. Having this interpretation in mind, and observing in Figure 12 that the upper price boundary premium is larger than the lower price boundary risk premium, one can conclude that sellers should pay more attention to seasonal model risk. The SMRP in Figure 13 takes on negative values because the seasonality reduces the futures prices below the price of model without seasonality. In particular, the absolute value of the upper price limit is larger than the absolute value of the lower price limit. This underlines the importance of properly modelling seasonality for sellers. Since financial institutions are likely to be the main sellers of wind power derivatives, the result provides an example of the importance of appropriate models of derivative pricing with seasonality by financial institutions.

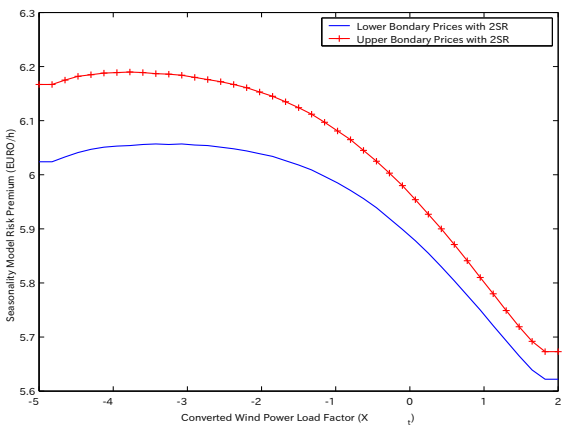

Figure 12. Seasonality model risk premium on December 31, 2017 for January 31, 2018 delivery. Note: Dax Note: Dax S_t is 11,400 as an example and $A = 2\phi$.

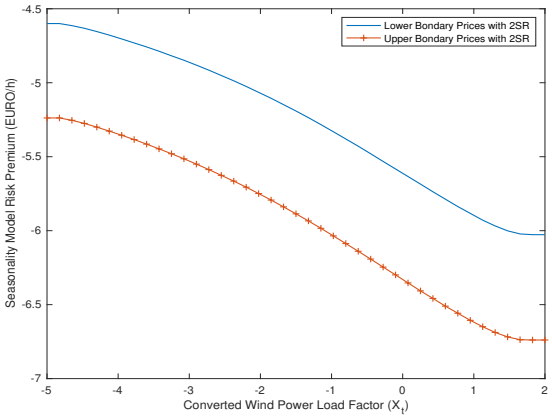

Figure 13. Seasonality model risk premium on June 30, 2018 for July 31, 2018 delivery. S_t is 11,400 as an example and $A = 2\phi$.

4.3. Applications

In this section, we discuss the applications of the results obtained in this study from three points of view. The results show, firstly, that the futures prices observed in the EEX market and the calculated futures prices are almost the same price level. As a robust model for wind power derivatives pricing, our pricing method can be applied to the pricing of new wind power derivatives, including the wind power options presented so far in this paper. The method can be applied to the development of tailor-made risk hedging products according to the risk hedging needs of wind power producers, e.g., a put option to hedge the risk of low wind power capacity utilisation and a call option to hedge the risk of wind power production restriction in case of overcapacity. In order to show the case of a put option, we design and price the following put option. We consider a European wind power put option with strike price K whose theoretical price $\underline{D}(S,X,I,T)$ based on a wind power futures as underlying is given by:

$$\underline{D}(S,X,I,T) = \max\left(K - \frac{I_T}{T}, 0\right). \tag{18}$$

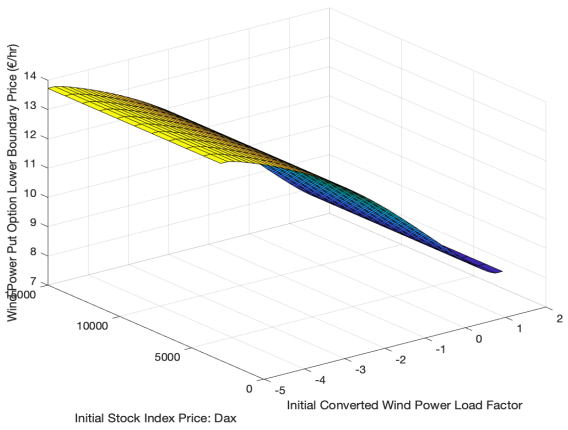

Figure 14. Wind power put option lower price boundary on December 31, 2017 for January 31, 2018 delivery. Note: $A = 3\phi$.

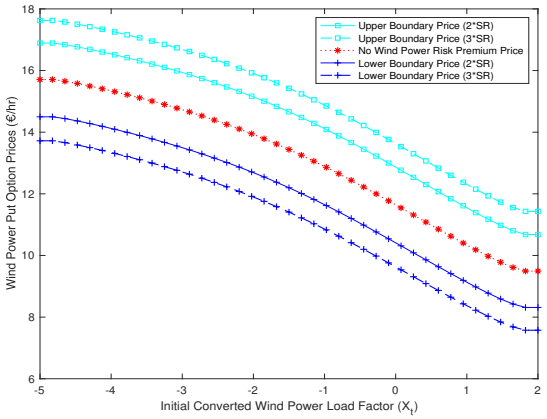

Figure 15. Wind power put option price boundaries on December 31, 2017 for January 31, 2018 delivery. Note: Dax S_t is 11,400 as an example.

Note $K = 0.45$ as an example. Figure 14 shows the lower boundary of the wind power put option price when the incomplete market demands three times the Sharpe ratio ($A = 3\phi$) in Equation (12). It can be seen that the impact of the initial stock price on the lower boundary of the wind power put option price is limited. Figure 15 shows the results for the case where the initial stock price is fixed at 11,400 and $A = \phi$ (No wind power risk premium), 2ϕ and 3ϕ, respectively. We additionally show an example of a wind power long strangle option which is used for a hedger who wants to hedge both the risk of low wind power capacity utilisation and the risk of wind power production restriction in case of overcapacity.

$$\underline{D}(S,X,I,T) = \max\left(K_1 - \frac{I_T}{T}, \frac{I_T}{T} - K_2, 0\right). \tag{19}$$

Note $K_1 = 0.3$ and $K_2 = 0.35$ as an example. Figure 16 shows the lower boundary of the wind power long strangle option price when the incomplete market demands three times the Sharpe ratio ($A = 3\phi$) in Equation (12). It can be seen that the impact of the initial stock price on the lower boundary of the wind power long strangle option price is limited. Figure 17 shows the results for the case where the initial stock price is fixed at 11,400 and $A = \phi$ (No wind

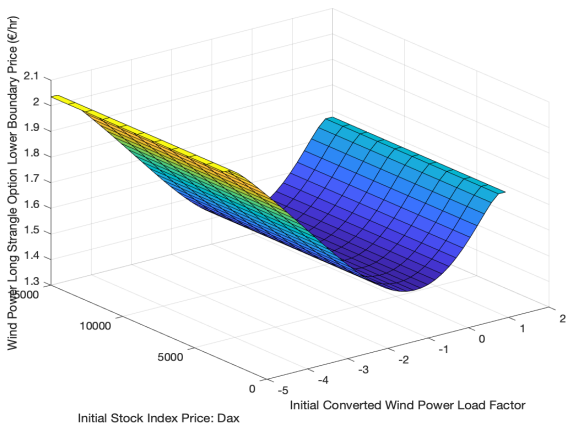

Figure 16. Wind power long strangle option lower price boundary with $K_1 = 0.3$ and $K_2 = 0.35$ on December 31, 2017 for January 31, 2018 delivery. Note: $A = 3\phi$.

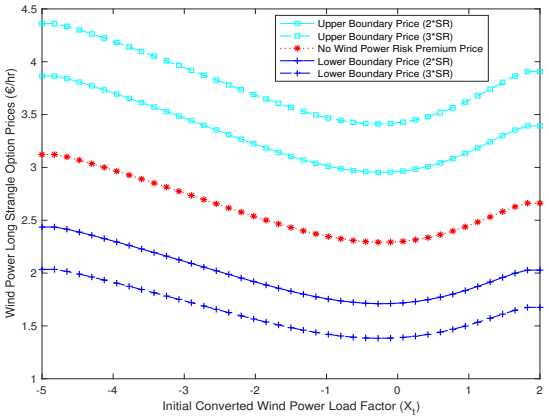

Figure 17. Wind power long strangle option price boundaries with $K_1 = 0.3$ and $K_2 = 0.35$ on December 31, 2017 for January 31, 2018 delivery. Note: Dax S_t is 11,400 as an example.

power risk premium), 2ϕ and 3ϕ, respectively. As one of the applied values of this research, considering the low liquidity of the wind power derivatives market, we were able to show practical examples of the design and pricing of a put option hedging the downward risk of wind power operation and a long strangle option hedging both the upward and downward risk of wind power operation.

The results of the present calculations show, secondly, that upper and lower boundaries can be obtained on the prices of wind power derivatives, reflecting the illiquidity of the wind power derivatives market. The upper boundary is considered to be the selling price and the lower boundary is considered to be the buying price, which can be applied to the derivation of the price in practice for each seller and buyer, respectively. If the seller of wind power derivatives is a financial institution and the buyer of wind power derivatives is a wind power producer, the upper price boundary obtained in this calculation is the selling price of the financial institution and the lower price boundary is the buying price of the wind power producer, respectively. In order to show the example, Table 8 reports the selling and buying prices of the call option valuation on December 31, 2017 for January 31, 2018 delivery and $A = 3\phi$ in Figure 9. As one

Initial Load Factor	0.8%	0.9%	1.1%	1.3%	1.6%	1.9%	2.2%	2.7%	3.2%
Seller's Price	11.201	11.263	11.346	11.437	11.535	11.637	11.744	11.856	11.973
Buyer's Price	7.197	7.247	7.315	7.392	7.475	7.562	7.654	7.750	7.852
Initial Load Factor	3.7%	4.4%	5.2%	6.2%	7.2%	8.5%	10.0%	11.7%	13.6%
Seller's Price	12.096	12.224	12.359	12.499	12.647	12.802	12.964	13.134	13.311
Buyer's Price	7.959	8.072	8.190	8.315	8.447	8.587	8.734	8.889	9.052
Initial Load Factor	15.8%	18.2%	21.0%	24.0%	27.4%	31.0%	34.9%	38.9%	43.2%
Seller's Price	13.497	13.690	13.892	14.102	14.319	14.543	14.773	15.010	15.251
Buyer's Price	9.224	9.405	9.594	9.792	9.999	10.214	10.437	10.667	10.904
Initial Load Factor	47.5%	51.9%	56.2%	60.5%	64.6%	68.5%	72.1%	75.5%	78.6%
Seller's Price	15.496	15.743	15.992	16.241	16.489	16.734	16.975	17.209	17.433
Buyer's Price	11.145	11.391	11.640	11.890	12.140	12.390	12.636	12.878	13.111

Table 8. Selling and buying prices of wind power call option on December 31, 2017 for January 31, 2018 delivery with Dax $S_t = 11,400$ and $A = 3\phi$

of the applied values of our research, we were able to show specifically the selling and buying prices of wind power derivatives using a wind power call option, reflecting the illiquidity of the wind power derivatives market.

Thirdly, the results show that the inclusion of seasonality in the modelling of the wind power index is important. In particular, the results show that sellers' prices represented by the upper price boundary are more affected by seasonality than buyers' prices represented by the lower price boundary. As a caution against the simplification of derivatives pricing in practice, the use of this sophisticated model with seasonality enables practitioners to have a beneficial application to wind power derivatives pricing. Particularly, the proposed model is more important when applied to financial institutions as sellers than to wind power companies as hedgers. In order to show the example, Table 9 reports the selling price differences obtained from the models with and without seasonality by using the result of the call option valuation on December 31, 2017 for January 31, 2018 delivery and $A = 3\phi$. This analysis in Table 9 shows that the seller, the financial institution, has mispriced this call option by approximately €6 by ignoring the seasonality of the underlying asset, which is considered as one of the applied values of our research.

Initial Load Factor	0.8%	0.9%	1.1%	1.3%	1.6%	1.9%	2.2%	2.7%	3.2%
Seller's Price Difference	5.711	5.731	5.754	5.778	5.801	5.823	5.845	5.867	5.889
Initial Load Factor	3.7%	4.4%	5.2%	6.2%	7.2%	8.5%	10.0%	11.7%	13.6%
Seller's Price Difference	5.912	5.934	5.956	5.977	5.998	6.018	6.038	6.057	6.074
Initial Load Factor	15.8%	18.2%	21.0%	24.0%	27.4%	31.0%	34.9%	38.9%	43.2%
Seller's Price Difference	6.089	6.103	6.115	6.124	6.131	6.135	6.136	6.133	6.127
Initial Load Factor	47.5%	51.9%	56.2%	60.5%	64.6%	68.5%	72.1%	75.5%	78.6%
Seller's Price Difference	6.117	6.103	6.087	6.066	6.042	6.016	5.987	5.955	5.923

Table 9. Selling price differences between the models with and without seasonality for wind power call option on December 31, 2017 for January 31, 2018 delivery with Dax $S_t = 11,400$ and $A = 2\phi$

5. Conclusions

In this paper, we analysed the theoretical prices of wind power derivatives under market incompleteness, and analysed the importance of seasonality modelling in this context as well as we showed the application of the theory to the practical implementation of the pricing with the illiquidity. There are two main obstacles to the pricing of wind power derivatives: the modelling of cash flows and the characterisation of stochastic discount factors in illiquid markets. In addition, the results of our empirical analysis are also of importance for other applications, such as enterprise risk management. As such, our study makes at least three contributions. Firstly, this paper contributes to the modelling of cash flows in the wind power derivatives sector. To the best of our knowledge, we conducted the first detailed econometric analysis of the underlying's time series, i.e., the electricity production from windmills in Germany, resulting in strong support of seasonality and mean reversion in the logit-transformed wind load factors. Based on the econometric findings, we propose a new wind load factor model for wind power derivatives in which the logit-transformed wind load factor follows a mean-reverting process in continuous time with seasonality. Second, this study contributes to the characterisation of stochastic discount factors in illiquid markets in the theoretical pricing of wind power derivatives. To conduct the pricing analytics of wind power derivatives, we apply

the good-deal bounds pricing methodology within the illiquid market situation to futures and call option contracts. Third, we provide a theoretical and empirical analysis on the importance of seasonality modelling for wind power futures. Our analysis shows that accurately capturing the seasonal aspects of the underlying series is crucial when pricing wind power derivatives. Our results further show that in both summer and winter, the absolute value of the upper price boundary of the risk premiums is larger than the absolute value of the lower price boundary. Given the interpretation that the upper and lower boundary represent the selling and the buying price in an incomplete market, the short position is more strongly affected by seasonality than the long position. Finally, as the discussions of the applications of the results in this paper we showed that three results in this paper, namely, the coherence between the calculation results and the EEX market observation results, the derivation of upper and lower price boundaries reflecting the illiquidity of the market, and the importance of seasonality in the calculation results, lead to the applicability of the proposed model to the development of tailor-made wind power risk hedging products, the applicability of the model to the derivation of prices for buyers and sellers of wind power derivatives, and the applicability of the model to the practice of financial institutions as the sellers, respectively.

Although the price analysis of wind power derivatives in this study is based on data from Germany, where the market for wind power and wind power derivatives is more advanced, it could well be extended to other countries, such as the US and Japan, if data, especially wind power derivatives data, are available. These empirical analyses will be the subject of future research, pending the development of the global wind derivatives market. The risk management of renewable energies including wind power has a comprehensive aspect that encompasses not only economic but also technical risks depending on the type of renewable energy. As can be seen from the wide range of journals in the reference of this paper from Energy Conversion and Management (Dorvlo, 2002; Akpinar and Akpinar, 2005; Bivona, Bonanno, Burlon, Gurrera, and Leone, 2011), Wind (Hennessey, 1978), and Journal of Applied Meteorology (Luna

and Church, 1974; Bardsley, 1980; Carlin and Haslett, 1982) as well as Energy Economics (Benth and Šaltytė Benth, 2009; Kanamura and Ōhashi, 2009; Lee and Oren, 2009; Gersema and Wozabal, 2017), the issue of modelling the risks of renewable energy should be seen as a category of applied energy, beyond the scope of energy economics. In future research on risk management of renewable energy for further promotion of renewable energy, it is important to discuss the issue in the field of applied energy, which is a multidisciplinary field with technical and applied aspects, not only in the existing category of energy economics.

Appendix A Further econometric analysis

For nearly every considered model we find evidence of ARCH-effects. This is indicated by the large number of significant Ljung–Box test statistics applied to the squared residuals. Inspecting the correlograms of the squared residuals suggests that there is not only annual seasonality in the mean of each series but also in the variance. During autumn and winter the variability in the wind power load factor increases, compared to summer and spring. The effect is more pronounced when the original data series is modelled. The data transformation helps to stabilise the variance and to diminish this effect, especially for the daily series.

Concerning the distributional assumption of the residuals, all models perform rather well. For the models applied to the weekly and monthly series the AD-test and the KPSS-test, both, do not reject normality. Only for the daily series does the AD-test find evidence for departures from the normal distribution for some models. The AD-test and the KPSS-test work similarly, but the AD-test is known to have larger power, which is enhanced by the very large sample size of the daily series and its subperiods. Thus, we can conclude that the AD-test correctly rejects, but only due to very small deviations from the normal distribution. To support this argument, the kernel density estimates and the QQ-plots of the model residuals are shown in Figure 18. For the ARMA(2,2) model applied to the daily series, the AD-test rejects at the 1%-

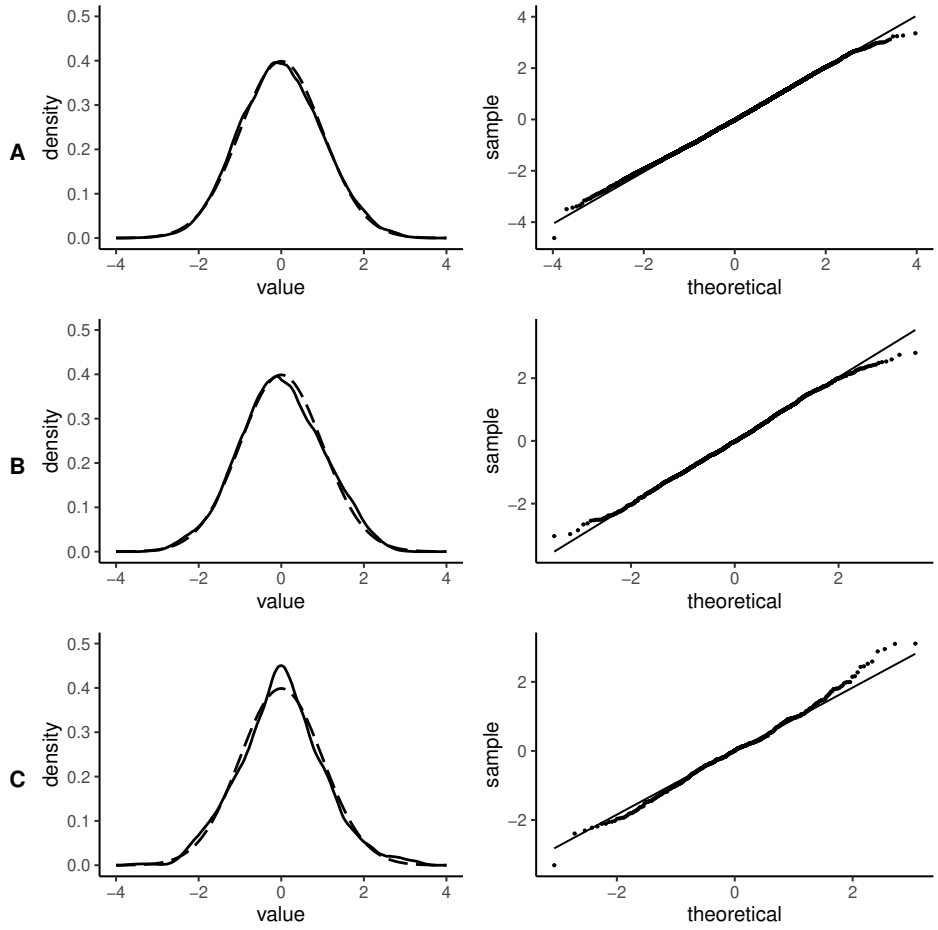

Figure 18. Kernel Estimate

This figure shows the kernel density estimate and the Q-Q-plot of the standardised residuals of the ARMA(2,2) and MA(1) fitted to the logit-transformed and deseasonalised series DWPLF and WWPLF, respectively, and of the logit-transformed and deseasonalised monthly series MWPLF. The Epanechnikov kernel is used with bandwidth following Silverman's rule. For reasons of comparison the normal density is printed in dashed lines.

significance level, whereas the KPSS does not reject. One can see that the density is following closely that of the normal distribution. The same holds for the models applied to the weekly and monthly series. We believe it is therefore reasonable to conclude that the estimated model describes the data sufficiently well. It is crucial to emphasise that the data transformation in Equation (1) is important for this to be the case. Depending on the application, it may have to be considered to model the found ARCH-effects.

References

Akpinar, E. K., and S. Akpinar, 2005, A statistical analysis of wind speed data used in installation of wind energy conversion systems, *Energy Conversion and Management* 46, 515–532.

Alexandridis, A., and A. Zapranis, 2013, Wind derivatives: Modeling and pricing, *Computational Economics* 41, 299–326.

Anderson, T. W., and D. A. Darling, 1952, Asymptotic theory of certain goodness of fit criteria based on stochastic processes, *Annals of Mathematical Statistics* 23, 193–212.

Bardsley, W. E., 1980, Note on the use of the inverse Gaussian distribution for wind energy applications, *Journal of Applied Meteorology* 19, 1126–1130.

Benth, F. E., L. Di Persio, and S. Lavagnini, 2018, Stochastic modeling of wind derivatives in energy markets, *Risks* 6, 1–21.

Benth, F. E., and A. Pircalabu, 2018, A non-Gaussian Ornstein-Uhlenbeck model for pricing wind power futures, *Applied Mathematical Finance* 25, 36–65.

Benth, F. E., and J. Šaltytė Benth, 2009, Dynamic pricing of wind futures, *Energy Economics* 31, 16–24.

Bessembinder, H., and M. L. Lemmon, 2002, Equilibrium pricing and optimal hedging in electricity forward markets, *Journal of Finance* 57, 1347–1382.

Bivona, S., G. Bonanno, R. Burlon, D. Gurrera, and C. Leone, 2011, Stochastic models for wind speed forecasting, *Energy conversion and management* 52, 1157–1165.

Brockett, P. L., M. Wang, C. Yang, and H. Zou, 2006, Portfolio effects and valuation of weather derivatives, *Financial Review* 41, 55–76.

Brown, B. G., R. W. Katz, and A. H. Murphy, 1984, Time series models to simulate and forecast wind speed and wind power, *Journal of Climate and Applied Meteorology* 23, 1184–1195.

Cao, M., and J. Wei, 2004, Weather derivatives valuation and market price of weather risk, *Journal of Futures Markets* 24, 1347–1382.

Carlin, J., and J. Haslett, 1982, The probability distribution of wind power from a dispersed array of wind turbine generators, *Journal of Applied Meteorology* 21, 303–313.

Cochrane, J. H., and J. Saa-Requejo, 2000, Beyond arbitrage: Good-deal asset price bounds in incomplete markets, *Journal of Political Economy* 108, 79–119.

Davis, M., 2001, Pricing weather derivatives by marginal value, *Quantitative Finance* 1, 1–4.

Dorvlo, A. S. S., 2002, Estimating wind speed distribution, *Energy Conversion and Management* 43, 2311–2318.

EEX, 2018a, EEX Final Settlement Price Wind Power Future January 2018, *https://www.eex.com/blob/78882/1ee80f2e68672a9d4adc6c04288554bf/20180131-customer-information—fsp-wind-power-future-january-2018-data.pdf*.

EEX, 2018b, EEX Final Settlement Price Wind Power Future July 2018, *https://www.eex.com/blob/84302/37216b1ac23765721f858e98724b6886/20180731-customer-information—fsp-wind-power-future-july-2018-data.pdf*.

Gersema, G., and D. Wozabal, 2017, An equilibrium pricing model for wind power futures, *Energy Economics* 65, 64–74.

Hennessey, J. P., 1978, A comparison of the Weibull and Rayleigh distributions for estimating wind power potential, *Wind Engineering* 2, 156–164.

Hess, M., 2021, A new model for pricing wind power futures, *Decisions in Economics and Finance, forthcoming*.

Kanamura, T., and Ōhashi, 2009, Pricing summer day options by good-deal bounds, *Energy Economics* 31, 289–297.

Kwiatkowski, D., P. C. B. Phillips, P. Schmidt, and Y. Shin, 1992, Testing the null hypothesis of stationarity against the alternative of a unit root: How sure are we that economic time series have a unit root?, *Journal of Econometrics* 54, 159–178.

Lee, Y., and S. S. Oren, 2009, An equilibrium pricing model for weather derivatives in a multi-commodity setting, *Energy Economics* 31, 702–713.

Ljung, G. M., and G. E. P. Box, 1978, On a measure of lack of fit in time series models, *Biometrika* 65, 297–303.

Luna, R. E., and H. W. Church, 1974, Estimation of long-term concentrations using a "universal" wind speed distribution, *Journal of Applied Meteorology* 13, 910–916.

Platen, E., and J. West, 2004, A fair pricing approach to weather derivatives, *Asia-Pacific Financial Markets* 11, 23–53.

Rodríguez, Y. E., M. A. Pérez-Uribe, and J. Contreras, 2021, Wind put barrier options pricing based on the Nordix index, *Energies* 14, 1177.

Sherlock, R. H., 1951, Analyzing winds for frequency and duration, in *On Atmospheric Pollution* (Springer) , 42–49.

Torres, A. Garciaand J. L., and E. Prietoand A. De Francisco, 1998, Fitting wind speed distributions: a case study, *Solar Energy* 62, 139–144.

Torres, J. L., A. Garcia, M. De Blas, and A. De Francisco, 2005, Forecast of hourly average wind speed with ARMA models in Navarre (Spain), *Solar Energy* 79, 65–77.

WindEurope, 2020, Financing and investment trends: The European wind industry in 2019, *https://windeurope.org/wp-content/uploads/files/about-wind/reports/Financing-and-Investment-Trends-2019.pdf*.